ACS ES&T Water

pubs.acs.org/estwater

Article

Effects of Hydrogen Peroxide on Cyanobacterium *Microcystis aeruginosa* in the Presence of Nanoplastics

Yawen Guo, Anna M. O'Brien, Tiago F. Lins, René Sahba Shahmohamadloo, Xavier Ortiz Almirall, Chelsea M. Rochman,* and David Sinton*

Cite This: *ACS EST Water* 2021, 1, 1596–1607

Read Online

ACCESS | Metrics & More | Article Recommendations | Supporting Information

ABSTRACT: Hydrogen peroxide (H_2O_2) is a common control measure for cyanobacterial harmful algal blooms (cyanoHABs), but local contaminants may alter its effects. Here, we aim to understand the control of cyanoHABs by H_2O_2 in light of nanoplastic contamination using a multistressor framework. We utilized a high-throughput full-factorial experiment to capture the multistressor impacts of H_2O_2, nanoplastics, temperature, and light on a toxigenic strain of the freshwater cyanobacterium *Microcystis aeruginosa*. In addition to revealing independent inhibitory effects of H_2O_2 and nanoplastics on cell abundance and microcystin production, our high-throughput system also identified non-additive, interactive effects. Specifically, we found that nanoplastics weakened the inhibitory effects of H_2O_2 on cell abundance and microcystin production. In addition, we discovered that nanoplastics restricted the degradation of H_2O_2, partially explaining this non-additive effect. Because combined H_2O_2 and nanoplastic still curbed growth, we expect H_2O_2 will remain an effective control measure even with background nanoplastic pollution. Our findings illustrate the importance of taking local stressors, including anthropogenic contaminants such as nanoplastics, into account before H_2O_2 is applied to control cyanoHABs.

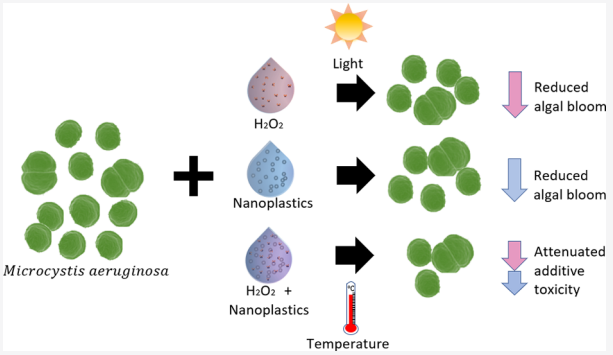

KEYWORDS: *cyanobacterial harmful algal blooms (cyanoHABs), chemical algaecide, water treatment, nanoplastics, multiple stressors, interactive effect*

INTRODUCTION

Cyanobacteria, also known as blue-green algae, naturally occur at low levels as a balanced planktonic assemblage in freshwater and marine ecosystems.[1,2] Certain conditions, especially anthropogenic nutrient inputs, can trigger rapid growth events known as cyanobacterial harmful algal blooms (cyanoHABs).[3] These blooms cause major problems for water quality, including reduced photosynthetic activity, and hypoxia or anoxia.[2,4] Moreover, some cyanobacterial species produce taste and odor compounds, and a variety of cyanotoxins that can cause liver, digestive, and neurological impairment when ingested by humans and animals.[3] Thus, watersheds affected by cyanoHABs have reduced utility for agricultural, aquacultural, recreational, and drinking water purposes.[5,6]

Several strategies for controlling or suppressing cyanoHABs exist, including reduction of nutrient inputs, hydrodynamic manipulations, ultrasonication, and chemical and biological controls.[2,5] Most physical methods have high costs and require coordinated action across the entire watershed, often necessitating national or international efforts.[2,7−9] Chemical algaecides are simpler to apply but persist over the long term and affect nontarget organisms, including eukaryotic phytoplankton, zooplankton, and fish,[10] and may actually increase the levels of cyanotoxins in water because the mode of action is cell lysis.[6,7] In contrast, the strong oxidant hydrogen peroxide (H_2O_2) decomposes into water and oxygen via chemical and biological pathways over a few hours or days,[11−13] leaving no long-term chemical traces, and has minimal nontarget effects: cyanobacteria are much more sensitive than eukaryotic phytoplankton, so very small doses can be effective.[9,14−17] Furthermore, H_2O_2 favors photocatalytic oxidation of cyanotoxins into nontoxic peptides, thus simultaneously controlling cyanoHABs and detoxifying water.[8,9,17] H_2O_2 is therefore widely used in water treatment and in the aquaculture industry.[8,18]

However, not all water bodies respond similarly, and the concentration of H_2O_2 needed to control cyanoHABs varies from 2 to 20 mg L^{-1}.[8,9,17,19] Varying background stressors in freshwater ecosystems may interact with H_2O_2, altering its

Received: March 15, 2021
Revised: June 4, 2021
Accepted: June 9, 2021
Published: June 17, 2021

efficacy in controlling cyanoHABs. Co-occurring stressors can have complex impacts on organisms and communities as stressors in combination can either amplify (synergistic) or attenuate (antagonistic) effects.[20−23] The variation of the dose of H_2O_2 required might therefore be linked to the growing number of background stressors faced by aquatic ecosystems, including a temperature increase, an elevated level of CO_2, and anthropogenic inputs such as pharmaceuticals, personal care products, pesticides, and, relevant to this study, tiny plastic fragments.[24,25]

Nanosized plastic particles, or nanoplastics (NPs), are expected to occur in essentially all ecosystems, including freshwater.[26−30] Nanoplastics are themselves of concern: their small size gives them high potential to penetrate tissue and cell membranes and may magnify toxic effects relative to larger pieces of plastic debris.[30−33] However, NPs may also interact with other environmental stressors, such as via adsorbing additional toxic heavy metals or organic pollutants onto their surfaces, altering their direct and bioaccumulated toxic effects.[29,34−39] Likewise, NPs could interact with H_2O_2 directly, resulting in an altered H_2O_2 concentration or NP aggregation behavior, or indirectly, if NPs modify the physiology, distribution, or behavior of cyanobacteria prior to H_2O_2 application and therefore influence their ability to tolerate H_2O_2. However, there has been a lack of investigation of either phenomenon, impeding forecasts of cyanoHAB responses to the application of H_2O_2 in local environments.

In this study, we explored the effect of H_2O_2 on a toxigenic strain of *Microcystis aeruginosa* in the presence of 100 nm polystyrene NPs. We investigated the individual influence of NPs, H_2O_2, and their combined effects on population abundance and microcystin production of *M. aeruginosa* across gradients of important ecological variables (light and temperature) over short-term exposure. To explore mechanisms underlying any interactive effects of NPs and H_2O_2, we quantified direct chemical or physical interactions between these two stressors prior to cyanobacterial exposure.

MATERIALS AND METHODS

Chemicals. We used fluorescently labeled amine-modified polystyrene (PS-NH_2) latex beads (100 nm; $\lambda_{ex} \sim 475$ nm; $\lambda_{em} \sim 540$ nm; Sigma-Aldrich) as NPs, which aided confocal microscopy observations. We focus on these particles because of their common usage in previous studies of the effects of nanoplastics on *M. aeruginosa*.[38,40,41] However, our particle source contained surfactants and biocides as additives, which may not be environmentally relevant. To circumvent the potential toxicity attributed to commercial additives on NPs,[32,42] we consecutively dialyzed the bulk of NPs for 5 days using a Micro Float-A-Lyzer device with dialysis membranes (molecular weight cutoff of 1000 Da) to leach out the additives. We performed material characterization of dialyzed polystyrene NPs using Raman spectroscopy (Horiba Scientific) of samples placed on a quartz slide and air-dried, and we verified the size and polydispersity of NPs before and after dialysis using dynamic light scattering [Wyatt DynaPro Plate Reader II (see for both ref 32)]. Environmentally relevant ranges for nanoplastics remain poorly characterized.[43−45] The concentration range that we selected for our study (5−100 mg L^{-1}, particles per liter calculation in the Supporting Information) covered the range of current potential and projected future concentrations in the aquatic environment, using the expectation that microplastics present in the environment at known concentrations[46,47] ultimately break down into nanoplastics (estimated by Lins et al., unpublished[48]). In addition, this range of nanoplastic concentrations covers the normal range for acute toxicity studies.[38,41,49,50]

The H_2O_2 solution [30% (w/w) in H_2O_2, containing stabilizer, Sigma-Aldrich] was stored in the refrigerator (4 °C, dark). A working stock solution at 3297.03 mg L^{-1} H_2O_2 was prepared using the 30% (w/w) H_2O_2 stock immediately before each experiment. The working stock solution was then added to mixtures of *M. aeruginosa* and NPs to reach final H_2O_2 concentrations of 0, 1, 5, and 20 mg L^{-1}, which covered relevant control application concentrations.[8,9,17,19] As H_2O_2 is not stable and susceptible to degrade into water and oxygen, a peroxide assay kit (MAK311, Sigma-Aldrich) and a PHERAstar FS microplate reader (BMG LABTECH, Germany) were used to ensure an accurate H_2O_2 concentration in each experiment and replicate.

Cyanobacterial Culture. *M. aeruginosa* strain CPCC 300 was provided by the Ministry of the Environment, Conservation and Parks (MECP, Toronto, ON). Following a previously described method, it was maintained in BG-11 medium in the 600 mL Falcon tissue culture treated flask at 24 ± 1 °C under full-spectrum 6400K fluorescence with a light illumination of 17 ± 2 μmol m^{-2} s^{-1} in a 16 h:8 h light:dark cycle.[51] *M. aeruginosa* is a bloom-forming genus of cyanobacteria, is widely distributed in mesotrophic to eutrophic freshwater worldwide, and releases the hepatotoxin microcystin.[16,51,52] *M. aeruginosa* CPCC 300 produces two variants, namely, microcystin-LR (MC-LR) and [D-Asp^3]-microcystin-LR (MC-dmLR). We scanned the absorbance spectra of a series of *M. aeruginosa* solutions at known densities from 300 to 800 nm in 2 nm increments using the BMG PHERAstar FS microplate reader (BMG LABTECH). We observed that optical density at 680 nm (OD_{680}) correlated linearly with cell density (Figure 4), and we fit calibration curves between cell density and OD_{680}, which we used to ensure a similar cell seeding density for experimental replicates (Figure S2). As *M. aeruginosa* cells are prone to deposit, we homogenized the liquid in each well by manually pipetting up and down several times carefully and then sealed the plates with an optical adhesive film (MicroAmp, Applied Biosystems) for OD measurement.

Preliminary Exposure of *M. aeruginosa* to Hydrogen Peroxide. To assess the suppression of *M. aeruginosa* by H_2O_2, we applied 0, 1, 5, 20, 40, and 60 mg L^{-1} H_2O_2 to *M. aeruginosa* at a seeding density of 3.00×10^6 cells mL^{-1} in full strength BG-11 medium and loaded 16 replicates of each mixture on a 384-well plate (Greiner CELLSTAR, catalog no. 781098). Subsequent changes in the optical density of *M. aeruginosa* and the corresponding H_2O_2 concentration of each treatment were monitored every 24 h consecutively for 3 days.

Experimental Device Setup. To prevent the evaporation of solutions in the well plates during the 72 h experiment and to ensure fresh air circulation within each well, we used a custom gas delivery device. Briefly, we placed an aerogel monolith over the open side of the experimental well plates and sandwiched both layers between a backplate on the closed plate surface and an acrylic layer with two channels above the aerogel. Each channel was connected with tubes that transported continuous humidified room air, and we set up three devices in parallel, with the same flow rate to each device (Figure S3).

https://doi.org/10.1021/acsestwater.1c00090
ACS EST Water 2021, 1, 1596−1607

We illuminated plates from below (three 6400K 24 W fluorescence lamps, brand Sun-Blaster) and manipulated light intensity with the distance of the light source, and optical adhesive films (MicroAmp, Applied Biosystems) applied to the bottom of the well plates, which we custom printed with four levels of a gray scale. We measured corresponding light intensities beneath each gray scale level on the printed film using a quantum meter (Li-COR) to confirm a linear correlation between the light intensity and the gray scale.[32] We compared the full absorbance spectrum of well plates with and without the printed films and found no significant difference in spectra, confirming only the intensity was changed.

To manipulate temperatures, we inserted devices (except the one exposed at room temperature) into an incubating chamber (Exo Terra PT2445) set at the desired temperature. Styrofoam pieces in the incubators were used to ensure an even temperature distribution throughout the apparatus and well plate, and a thermocouple immersed inside the wells at opposite ends was used to monitor the temperature during the experiment. The temperature difference across each plate (i.e., from one side of the plate to the other) was kept within 1 °C.

Effects of Testing of Hydrogen Peroxide and Nanoplastics on *M. aeruginosa* across Environmental Conditions. For each run of the experiment, we combined six concentrations of polystyrene NPs, four concentrations of H_2O_2, three levels of temperature, and four levels of light intensity in a full-factorial design. First, we mixed *M. aeruginosa* cultures at a cell seeding density of 1.5×10^6 with dialyzed PS-NH_2 and H_2O_2 to reach the final NP mass concentrations of 0, 10, 30, 50, 70, and 100 mg L^{-1} and H_2O_2 concentrations of 0, 1, 5, and 20 mg L^{-1}, keeping the BG-11 background full strength across treatments. Our initial cell density is between the World Health Organization limits for a cyanobacterial bloom with potential for causing long-term illness (10^5 cells mL^{-1}) and one that would cause severe health outcomes (10^7 cells mL^{-1}).[1,53] We then loaded the respective *M. aeruginosa*/NPs/H_2O_2 mixtures into the 384-well plates (Greiner CELLSTAR, 781098) with a total volume of 100 μL per well. We chose white 384-well plates to reduce light crosstalk between wells and to avoid any loss of light intensity reaching the culture. We sealed the well plates with a breathable membrane (Diversified Biotech Breathe-easy) and inserted into devices as described above.

Light intensities were 13 ± 2, 17 ± 2, 21 ± 2, and 27 ± 2 μmol m^{-2} s^{-1}, simulating the range of light levels from the surface to underwater,[54] and within the range of irradiance that affects cell growth and microcystin production.[55−57] Temperature levels were 18 ± 1, 24 ± 1, and 30 ± 1 °C, covering the range of variation among locations, weather events, seasons, and water column locations.[58,59] In total, we were able to incorporate 288 unique treatment combinations with four internal replicates per run of the experiment. All runs lasted 72 h, and we replicated the full set of treatments in five runs (five independent runs, and four replicates per run, yielded 20 wells × 288 treatments; degrees of freedom = 5759).

***M. aeruginosa* Growth and Microcystin Synthesis.** Cell density after the 72 h exposure experiment was determined by measuring the optical density at 680 nm (OD_{680}) and the calibration curves (Figure S2). We subtracted the adsorption of NP particles in the culture medium at the same wavelength for background adjustment. We then covered plates with AluminaSeal and stored them at −20 °C. We randomly chose three replicates of the total of five and selected 16 treatments of the 288 to cover the lowest and highest values of each parameter for microcystin measurements: 0 and 20 mg L^{-1} for H_2O_2, 0, 100 mg L^{-1} for PS-NH_2, 18 and 24 °C for temperature, and 13 and 27 μmol m^{-2} s^{-1} for light intensity.

More than 250 microcystin congeners have been identified, but MC-leucine-arginine types are the most common and harmful ones.[60,61] We quantified the two microcystin variants (MC-LR and MC-dmLR) produced by the CPCC 300 strain using an automated online solid phase extraction coupled to liquid chromatography-quadrupole time-of-flight high-resolution mass spectrometry (Xevo G2-XS, Waters, Milford, MA).[62] In brief, selected *M. aeruginosa* samples were frozen and thawed for three cycles to lyse the cells so that microcystins would be free in solution. Then the samples were centrifuged at 3000*g* for 5 min to remove dead cell debris. Fifty microliters of the supernatant was diluted with 495 μL of reverse osmosis water and 15 μL of nodularin (0.5 μg L^{-1}) as an internal standard. Samples were syringe filtered (13 mm, 0.2 μm, GHB membrane) into separate 2 mL autosampler vials, and a 500 μL aliquot was injected.

Investigating the Sources of the Effects of Nanoplastics and Hydrogen Peroxide. We evaluated the effect of H_2O_2 on the particle size distribution and aggregation of PS-NH_2 by measuring the hydrodynamic diameter. We mixed three levels of PS-NH2 (50, 100, and 150 mg L^{-1}) with three H_2O_2 concentrations (0, 5, and 20 mg L^{-1}) factorially in 200 μL of BG-11 medium, which was filtered through a 0.22 μm membrane before being used to remove large proteins. The nine solutions were then loaded in a black 96-well plate (Corning, catalog no. 3615) and placed under light illumination (17 ± 2 μmol m^{-2} s^{-1}) in a 16 h:8 h light:dark cycle. We included three replicates for each treatment combination. After exposure for 24 h, we sent these 27 samples to compare their hydrodynamic diameters via dynamic light scattering (DLS) measurement using a DynaPro Plate Reader II (Wyatt Technology) at 23 °C.

To measure the impact of polystyrene NPs on the degradation of H_2O_2, we incubated two concentrations of H_2O_2 (5 and 20 mg L^{-1}) with four PS-NH_2 levels (0, 50, 100, and 150 mg L^{-1}) factorially with three replicates in 200 μL of BG-11 medium under the same exposure conditions described above. After 24 h, we detected the remaining H_2O_2 concentration in each well by a peroxide assay using the BMG PHERAstar FS microplate reader (BMG LABTECH). The change in H_2O_2 concentration = $C_1 - C_0$, where C_0 and C_1 are the H_2O_2 concentrations in mixtures at times t_0 (before experiment, day 0) and t_1 (after 24 h experiment, day 1), respectively.

Statistical Analysis. For each experiment, we used JMP Pro to fit separate general linear regression models, testing relationships between each response (dependent variable) and all manipulated (independent) variables and including random effects for replicated experimental runs. Dependent variables were the OD value for the preliminary exposure experiment, the cell density and concentration of microcystins for the multistressor experiment, and the hydrodynamic diameter and remaining H_2O_2 concentration for the source of effects experiment. Independent variables were H_2O_2 levels for the preliminary exposure experiment; NPs, H_2O_2, light, and temperature for the multistressor experiment; and NPs and H_2O_2 for the source of effects experiment. We rescaled each response variable to range from −1 to 1 to improve model

https://doi.org/10.1021/acsestwater.1c00090
ACS EST Water 2021, 1, 1596−1607

fitting. For each response variable, the fitted model included all main and interactive effects among independent variables (models with all terms are listed in Tables 1 and 2 and Tables S1 and S2, except the preliminary exposure model, in which the only independent variable was the H_2O_2). The *F* ratio and Prob > *F* statistics tested the significance of each term in the model. We considered a Prob > *F* value of <0.05 as significant. To verify and visualize complex interactive effects in the full-factorial experiment, we refit the relationship between H_2O_2 and cell density for each unique combination of light, temperature, and NPs treatments in Python using the seaborn package.[63,64]

Table 1. Summary Statistics for the Linear Regression Model of the Full-Factorial Experiment for the Effects of Four Factors (H_2O_2, Nanoplastics, Light, and Temperature) and Their Full-Factorial Interactions on *M. aeruginosa* Abundance

term	estimated coefficient	*F* ratio	Prob > *F*
H_2O_2	−0.909	3601.92	<0.0001
nanoplastics	−0.992	3380.90	<0.0001
temperature	0.208	164.68	<0.0001
light	0.050	7.83	0.0051
H_2O_2 × nanoplastics	0.612	984.80	<0.0001
temperature × H_2O_2	0.262	200.21	<0.0001
temperature × light	0.126	33.13	<0.0001
temperature × nanoplastics	0.100	23.07	<0.0001
H_2O_2 × light	0.055	7.21	0.0073
nanoplastics × light	0.049	4.53	0.0334
temperature × H_2O_2 × nanoplastics	0.106	19.68	<0.0001
temperature × nanoplastics × light	0.075	7.17	0.0074
temperature × H_2O_2 × light	0.061	5.90	0.0152
H_2O_2 × nanoplastics × light	0.061	5.44	0.0197
temperature × H_2O_2 × nanoplastics × light	0.021	0.41	0.5222

Table 2. Summary Statistics for the Linear Regression Model of the Experiment for the Effects of Nanoplastics, Initial H_2O_2, and Their Interactions on the Change in H_2O_2 Concentration

term	estimated coefficient	*F* ratio	Prob > *F*
initial H_2O_2	−1.96	49.53	<0.0001
nanoplastics	0.86	8.86	0.0036
initial H_2O_2 × nanoplastics	0.77	4.59	0.0345

Confocal and Scanning Electron Microscopy. A confocal laser scanning microscope (CLSM, Zeiss LSM 880 Elyra Superresolution) was used to observe the interactions between our fluorescent nano PS-NH_2 beads and *M. aeruginosa* cells. Ten milliliters of a culture with 2 × 10^6 cells mL^{-1} was exposed to fluorescent PS-NH_2 beads at 10 mg L^{-1} and maintained at room temperature under 17 ± 2 μmol m^{-2} s^{-1} illumination in a 16 h:8 h light:dark cycle for 72 h. An aliquot of the solution was sampled at the end of exposure and fixed with 4% paraformaldehyde with 1% glutaraldehyde in 0.1 M phosphate buffer (pH 7.2) at 4 °C for 48 h. The excitation wavelength of the laser source was 488 nm, and the bands for the emission filters were split into 493−556 and 568−712 nm channels.

Scanning electron microscopy (SEM, FEI XL30) observations were performed to investigate potential external interactions between NPs and *M. aeruginosa*. After exposure to 10 mg L^{-1} PS-NH_2 beads for 72 h under the same conditions of light, temperature, and *M. aeruginosa* cell density that were used for confocal microscopy, the samples were fixed in 2% glutaraldehyde in 0.1 M sodium cacodylate buffer (pH 7.3) at 4 °C overnight. The samples were washed for 20 min in 0.1 M sodium cacodylate buffer (pH 7.3) with 0.2 M sucrose (pH 7.3) and postfixed with 1% OsO_4 in 0.1 M sodium cacodylate buffer (pH 7.3) for 1.5 h. The samples were then dehydrated in a graded ethanol series (70, 90, and 100% × 3; 10 min each) and washed again for 20 min in 0.1 M sodium cacodylate buffer (pH 7.3) with 0.2 M sucrose (pH 7.3). After dehydration, the samples were desiccated in a critical-point dryer (Bal-Tec CPD 030). Finally, samples were coated with gold using a sputter coater (Leica EM ACE).

RESULTS

Effect of Hydrogen Peroxide on *M. aeruginosa* Abundance. Higher concentrations of H_2O_2 were toxic to

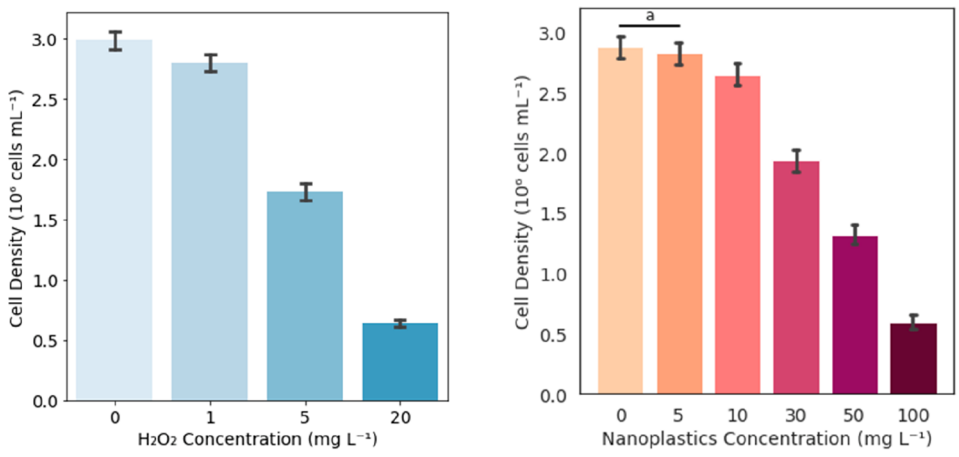

Figure 1. Averaged cell density of *M. aeruginosa* in each (a) H_2O_2 and (b) PS-NH_2 bead treatment after exposure for 72 h. Each bar is the mean of all data in each treatment. Error bars show ±1 standard error of the mean.

https://doi.org/10.1021/acsestwater.1c00090
ACS EST Water 2021, 1, 1596−1607

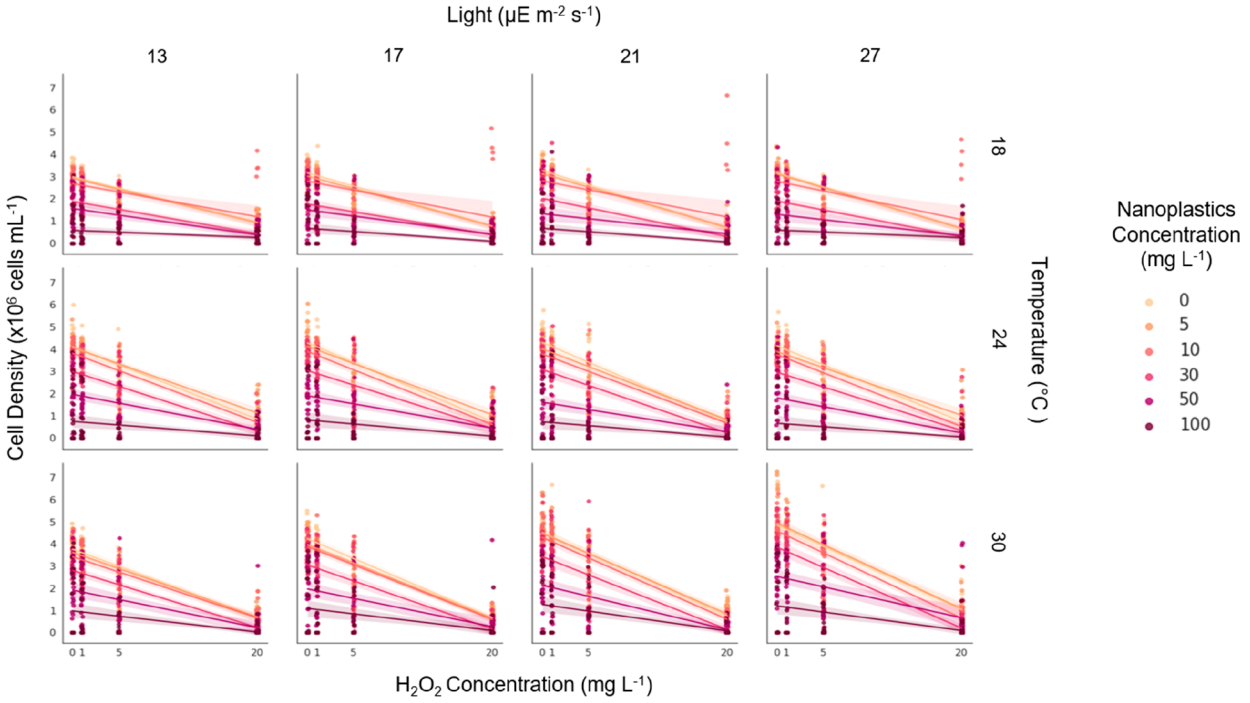

Figure 2. Cell density of *M. aeruginosa* after exposure for 72 h showing the interactive effects of H_2O_2 (0, 1, 5, and 20 mg L^{-1}, *x*-axis), light (13, 17, 21, and 27 μmol m^{-2} s^{-1}, across columns), temperature (18, 24, and 30 °C, across rows), and nanoplastics [0 (yellow), 5, 10, 30, 50, and 100 (red) mg L^{-1}; intermediate levels in intermediate colors]. Lines (mean) and shaded areas (95% confidence interval) represent linear models and expectations for cell density, fitted for each treatment combination separately.

M. aeruginosa in our 384-well plate experiments (Figure S4). Application of H_2O_2 at 20, 40, and 60 mg L^{-1} inhibited cell density by 65.1%, 71.8%, and 73.7%, respectively, compared with the control value after exposure for 3 days. In contrast, the treatment with ≤5 mg L^{-1} H_2O_2 only slightly suppressed population growth throughout the experiment.

H_2O_2 decayed less over time in *M. aeruginosa* cultures when applied in large doses (Figure S5). The concentration of H_2O_2 in the treatments with an initial dose of 5 mg L^{-1} decayed to <10% within 24 h. In contrast, the H_2O_2 concentration in 60 mg L^{-1} treatments decayed to only 70% in the first 24 h. After 24 h, H_2O_2 concentrations remained steady for the remaining time.

Combined Effects of Nanoplastics, Hydrogen Peroxide, and Environmental Parameters on *M. aeruginosa* Abundance. *Main Effects of Each Variable.* Our linear regression model with more than 5000 raw data points (model 1) enabled us to investigate the relationship between cyanobacterial cell density and multiple stressors. H_2O_2 had the most significant inhibitory effects [Prob > *F* is <0.0001 (Figure 1a)]. The cell densities of *M. aeruginosa* with 5 and 20 mg L^{-1} H_2O_2 after exposure for 72 h were 57.8% and 22.9%, respectively, of that of the control conditions. Nanoplastics also had a dose-dependent inhibitory effect on cyanobacteria, ranking as the second most important factor according to *F* ratio in Table 1 (Prob > *F* is <0.0001). Cell density was not significantly affected by 5 mg L^{-1} PS-NH_2 but was 68.4%, 50.0%, and 30.6% of NP-free treatments with 30, 50, and 100 mg L^{-1} PS-NH_2, respectively (Figure 1b). An increased temperature promoted cyanobacterial growth, consistent with previous studies, in which the optimum growth rate of *M. aeruginosa* was found to be around 30−32 °C.[56,65,66] The effects of light were not as evident (Table 1; Prob > *F* is around 0.005), possibly due to the low (but representative of natural conditions) light intensities in this experiment.

Interactive Effects between Variables. As described above, both NPs and H_2O_2 inhibited the growth of *M. aeruginosa*. However, the sign of the coefficient of the two-way interaction term was positive, implying an antagonistic interaction between NPs and H_2O_2 such that the net impact of PS-NH_2 and H_2O_2 on *M. aeruginosa* abundance was less than the sum of their independent effects. Indeed, the independently fitted slopes of relationships between cell density and H_2O_2 were also less steep at the higher nanoplastic concentrations (Figure 2). The reduction in the cyanobacterial cell density with 20 mg L^{-1} H_2O_2 alone or 100 mg L^{-1} NPs alone compared to the treatments without either stressor was 3.26×10^6 or 3.16×10^6 cells mL^{-1}, respectively, but the reduction was only 3.33×10^6 cells mL^{-1} with both 100 mg L^{-1} NPs and 20 mg L^{-1} H_2O_2 (averaged across all temperature and light levels).

The sub-additive inhibition of cell growth may be due to the acute toxicity of the highest NP (100 mg L^{-1}) or H_2O_2 (20 mg L^{-1}) levels alone; the cell density was almost zero under these conditions, such that the addition of the second chemical cannot trigger any further effect. Indeed, effect sizes were more consistent on the relative scale: the percentage reduction in cyanobacterial cell density with a dose of 20 mg L^{-1} H_2O_2 was 78.8% for groups without NPs and 83.2% for groups with the highest NPs, even though the absolute effect on cell density was much smaller at the highest NP level. Thus, we retested this interactive effect when excluding data from the highest level of both NPs and H_2O_2. As shown in Table S1, the interaction term between NPs and H_2O_2 was still positive, and the signs of their individual terms were both negative; however, they were smaller in magnitude compared to the same terms in model 1 [see also smaller differences among slopes (Figure 2 and Figure S6)]. Indeed, the percentage reduction in

https://doi.org/10.1021/acsestwater.1c00090
ACS EST Water 2021, 1, 1596−1607

cyanobacterial cell density compared with the control group was 35.8% for groups with 5 mg L^{-1} H_2O_2 without NP and 52.9% for treatments with 50 mg L^{-1} NPs without H_2O_2. However, when these second-highest levels of H_2O_2 and NPs were simultaneously applied, the cyanobacterial cell density was only reduced by 74.5% (lower than the additive expectation of 88.7%; percentages are across all temperature and light levels). The significant non-additive responses in cell density found with the full range of NPs and H_2O_2 were therefore partially due to the acute toxicity induced by a large dose of either chemical.

In contrast, higher temperatures amplified the negative effects of both H_2O_2 and NPs on cyanobacterial cell density (Table 1; both Prob > *F* values are <0.0001). Within each NP level, the decline in cell density across H_2O_2 concentrations was more pronounced at higher temperatures [steeper slopes in the bottom row vs the top row (Figure 2)]. Higher temperatures also strengthened the positive effects of brighter light [Table 1; Prob > *F* is <0.0001; intercepts of matching-color lines in the top left to bottom right panels (Figure 2)]. Indeed, light and sufficiently high temperatures are both required to increase the rates of photosynthesis of *Microcystis* spp.[56]

The interactions between H_2O_2 and light and those between NPs and light were nonsignificant (Prob > *F* values of 0.0073 and 0.0334, respectively). Three-way and higher interaction terms were mostly not significant, except the "Temperature × H_2O_2 × Nanoplastics" term (Table 1), which suggested that the combined effects of H_2O_2 and NPs on cyanobacterial abundance were the least additive at high temperatures (larger differences in slope among lines within panels in bottom vs top panels of Figure 2).

Effects on Microcystin Production. The individual and combined effects of multistressors on the total MC-LR and MC-dmLR concentration, as assessed by our linear regression model, were weaker than those observed for the cell density model (Table S2, model 2). Similar to the results for growth (Table 1, model 1), H_2O_2 and NPs were ranked (*F* ratio) as the first and second most critical parameters, respectively, in explaining total MC-LR and MC-dmLR production after exposure for 72 h (Prob > *F* is <0.0001), and both stressors had dose-dependent inhibitory effects on MC-LR and MC-dmLR. The positive sign of the "H_2O_2 × Nanoplastics" term captured the fact that the cumulative effects of the two stressors on MC-LR and MC-dmLR generation and production were less than the additive. Without NPs, adding 20 mg L^{-1} H_2O_2 reduced the total MC-LR and MC-dmLR concentrations by 68.9%; however, with 100 mg L^{-1} NPs, adding 20 mg L^{-1} H_2O_2 reduced the total MC-LR and MC-dmLR concentrations by 25.4%. Furthermore, at 20 mg L^{-1} H_2O_2, there was no additional reductive effect of 100 mg L^{-1} NPs on microcystin concentrations (Figure 3 and Figure S7).

Possible Mechanisms of Interactive Effects between Nanoplastics and Hydrogen Peroxide. We measured the aggregation behavior of PS-NH_2 by measuring hydrodynamic diameters (D_h), which increase as particles aggregate. H_2O_2 showed no significant effect on the aggregation of PS-NH_2 (Figure S8). Because no differences in NP aggregation at different H_2O_2 concentrations were observed, the influence of H_2O_2 on the aggregation of NPs cannot explain the interactive effects.

We also measured H_2O_2 decomposition rates across concentrations of PS-NH_2. Nanoplastics inhibited the degradation of H_2O_2 in the media, as illustrated by the positive linear model coefficient, implying less H_2O_2 was consumed (Table 2, model 3). Hydrogen peroxide in media without NP degraded the most within this time frame, and with a concentration of 150 mg L^{-1} PS-NH_2, only approximately half as much H_2O_2 was consumed (Figure S9). At higher initial H_2O_2 concentrations, the degradation rate of H_2O_2 was also higher [significantly negative coefficient (Table 2)].

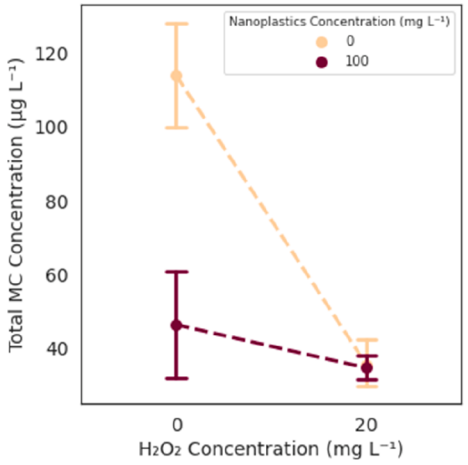

Figure 3. Total microcystin (MC-LR + MC-dmLR) concentrations after exposure for 72 h showing the combined effects of nanoplastics (0 and 100 mg L^{-1}) and H_2O_2 (0 and 20 mg L^{-1}) across all light (13 and 27 μmol m^{-2} s^{-1}) and temperature (18 and 30 °C) conditions. The 95% confidence intervals are shown.

We briefly explored how well this result could describe the full interactive effect of NPs and H_2O_2 on *M. aeruginosa* abundance by using the regression formula of model 3 to predict the amount of H_2O_2 lost in each treatment (extrapolating effects across the full ranges of concentrations), substituting this for the original variable "H_2O_2" and excluding the nanoplastics and H_2O_2 interactions from the model 1, and comparing the fits. As the exposure time of the H_2O_2 degradation study was 24 h, but that of the cell density study was 72 h, we assumed the amount of H_2O_2 consumption within 72 h was identical to that of 24 h, as we observed that most changes in concentration took place within 24 h (see Effect of Hydrogen Peroxide on M. aeruginosa Abundance). The modified model (AICc 14531.2) fit better than the original model excluding the nanoplastics and H_2O_2 interactions (AICc 15055.3) but worse than the full original model (model 1, AICc 14158.9), implying that the comprehensive interaction of NPs and H_2O_2 could be only partially explained by the effect of NPs on H_2O_2 decomposition, at least as estimated by our methods.

Interactions between Nano PS-NH_2 Beads and *M. aeruginosa*. To explore why NPs affect cyanobacterial growth, the effects of NPs on cell morphology and structure were examined by microscopy. Confocal laser scanning microscopy observations illustrated that the 100 nm PS-NH_2 beads adhered to the external surface of *M. aeruginosa* (Figure 4a,b), and a series of images taken at different three-dimensional slices revealed that a few NP beads entered cyanobacterial cells (Figure S11). Similarly, SEM showed that some nano PS-NH_2 particles agglomerated with each other and adsorbed on the surface of *M. aeruginosa* (Figure 4d).

https://doi.org/10.1021/acsestwater.1c00090
ACS EST Water 2021, 1, 1596−1607

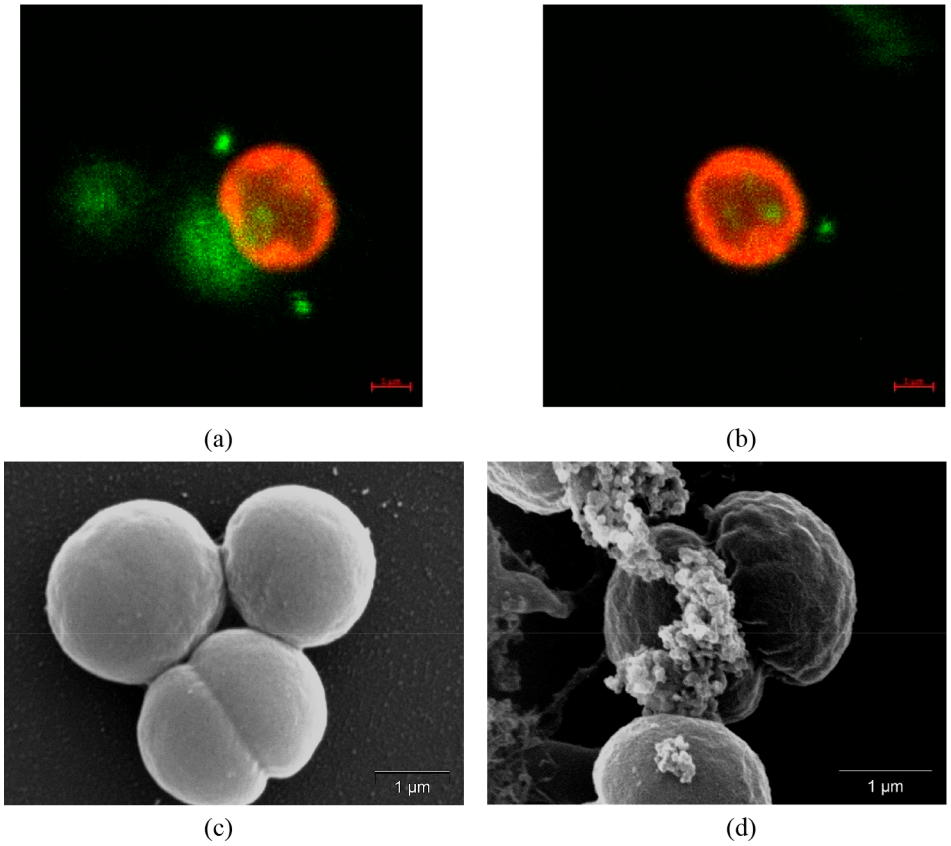

Figure 4. (a and b) Confocal microscopy images of *M. aeruginosa* cells showing the adhesion of PS-NH_2 on the surface, after incubation for 72 h at 10 mg L^{-1}. Green fluorescence corresponds to PS-NH_2 beads, and red fluorescence to autofluorescent *M. aeruginosa*; (c and d) SEM images of the interaction between 100 nm PS-NH_2 (10 mg L^{-1}) and *M. aeruginosa* after incubation for 72 h. (c) *M. aeruginosa* without PS-NH_2 (25000×). (d) PS-NH_2 adsorbed on *M. aeruginosa* cells (25000×).

DISCUSSION

Cyanobacterial harmful algal blooms are a growing issue, with impacts on ecosystem services and human health. Hydrogen peroxide is a popular control mechanism, but the required dose varies across sites, possibly in part due to environmental conditions and background contaminants. Polystyrene is one of the most widely used plastics worldwide, and small fragments of micro- and nanosized polystyrene particles have been detected in various aquatic ecosystems and wastewater discharge.[50,67] Also, positively charged micro- and nanoplastics are shown to induce more severe detrimental effects on tested organisms compared with uncharged and negatively charged ones in both short-term and long-term exposure studies.[40,50,68−70] Here, we tested how H_2O_2 control of cyanoHABs and the associated toxicity may be affected by a background of positively charged polystyrene NPs across other environmental conditions.

We discovered dose-dependent suppression of cyanobacterial abundance and toxicity caused by H_2O_2 and NPs (Table 1 and Table S2). The adherence of aggregated NP particles to cyanobacterial cell surfaces (Figure 4) suggests that the NP toxicity we observed may derive from physical blockage of light, nutrients, and gas flow, suppressing mitochondrial metabolism and increasing the level of intracellular reactive oxygen species (as reported previously[71−73]). We did not detect cell morphology abnormalities with SEM, but confocal imaging illustrated the cellular uptake of NPs (Figure S11), suggesting that NPs could alternatively or additionally have internal effects. We suggest that further elucidating the mechanism of NP effects might provide useful information for the development of new cyanoHAB control measures, such as documenting the presence, timing, or manner of any reactive oxygen species (ROS) response. In contrast to a previous study in which exposure to 50 nm PS-NH_2 promoted microcystin synthesis,[40] we found that 100 nm PS-NH_2 exerted a negative effect on MC-LR and MC-dmLR production. This discrepancy could be explained by the different strains of *M. aeruginosa* and/or the different sizes of PS-NH_2 beads used, which may change its toxicity, uptake threshold, and retention time.[71,74−76] Indeed, other properties that vary across nanoplastics, including shape, parent material, or surface charge, could alter biological effects, and we recommend these sources of variation be given greater consideration in future research. For example, our particles are likely to have been positively charged,[38,40,77] but particles vary in charge in the environment,[78−80] with negatively charged particles often having weakened biological effects.[40,72,81] Therefore, our results may represent stronger than average effects of nanoplastics on cyanoHAB control.

Interactions among NPs, H_2O_2, temperature, and light were significant predictors of *M. aeruginosa* cell growth (Table 1). We found that NPs reduced the effect of H_2O_2 on both growth and microcystin generation, resulting in lower-than-expected cumulative toxicity (Table 1, Table S2, Figures 2 and 3, and Figure S7). Thus, estimation of the H_2O_2 dose needed for efficient cyanobacterial bloom management should take into account the background NP level in the local aquatic

https://doi.org/10.1021/acsestwater.1c00090
ACS EST Water 2021, 1, 1596−1607

environment, as applying the same dose as another water body could result in insufficient H_2O_2 to curb a local cyanoHAB. Nontarget organisms might not have the same responses as cyanobacteria to H_2O_2 treatment in a background of NPs, and if instead NPs and H_2O_2 additively or synergistically harm nontarget organisms, other control mechanisms might need to be considered. We recommend that research going forward consider other environmental variables that could interactively alter the effects of NPs or cyanoHAB control measures, such as suspended sediments and organic matter.[82−86]

A similar result of sub-additive effects was observed in a study of the combined toxicity of nano PS-NH_2 and glyphosate on *M. aeruginosa* growth.[38] Several meta-analyses revealed that antagonistic interactions between stressors frequently occur in aquatic environments and may be commonly due to the nature of biological stress responses.[21,87−91] Indeed, we found that the sub-additive inhibition of cell growth may be partly, but not exclusively, due to the acute toxicity of the highest NP (100 mg L^{-1}) or H_2O_2 (20 mg L^{-1}) levels restricting any further biological response to additional stressors (Table S1).

Antagonistic interactions between stressors can also be due to direct interactions, which appear to contribute to this system, as we found a slower H_2O_2 degradation rate when NPs were present. It is the decomposition of H_2O_2 that causes biological toxicity: free hydroxyl radicals arise upon decomposition, which hinder photosynthetic activity and trigger oxidation of biomolecules, causing the cell death and microcystin cleavage in *M. aeruginosa*.[14,17,92,93] Thus, a slower degradation rate is consistent with reduced toxicity to algae. We suggest that the cause of this decreased H_2O_2 degradation rate is the increased turbidity at higher concentrations of NPs, which may block, absorb, and scatter some part of incident light onto the system.[94,95] Increasing NP concentrations in the solution induce more loss of irradiance (Figure S10), impeding the breakdown of H_2O_2. Our comparison of separate regression models including either experimentally manipulated H_2O_2 inputs or the extrapolated H_2O_2 loss or irradiance loss replacing NPs (also see the calculation of the relative loss of irradiance in the Supporting Information) further supports this proposed mechanism, although these tests include a few assumptions, such as no impact of manipulated temperature and light levels on H_2O_2 degradation.

Only higher temperatures and brighter light increased the rate of cyanobacterial growth in our experiments. This is not surprising because several species of cyanobacteria are known to grow faster in warmer waters,[56,96−98] and/or under higher irradiance,[56,99−101] and the scope of temperature and light levels that we chose was within the range of those in the literature. In addition, we found increasing temperature partially mitigated the negative effects of NPs on cell growth (Table 1 and Figure 2), similar to effects observed for a marine alga in Yang et al.[32] Interestingly, this relationship suggests that NP pollution could reduce the rate of proliferation of harmful algal blooms during warmer weather. As reported in previous studies, microcystin concentrations were not correlated with *M. aeruginosa* biomass, and the diverse effects of light and temperature on microcystin production reported in the literature seem to depend on the cyanobacterial strains and species and the microcystin analogue,[56,102−105] possibly explaining why we did not capture any effects of temperature or light on microcystin production.

CONCLUSION

In summary, this study provides a comprehensive test of the combined effect of H_2O_2 and polystyrene nanoparticles on the growth of the freshwater cyanobacterium *M. aeruginosa* in a short-term exposure across a range of environmental conditions. Our results support our hypothesis that the combined effects of H_2O_2 and NPs are different from those when in isolation, and there is an antagonistic effect of these two variables, such that their simultaneous application reduces *M. aeruginosa* abundance and microcystin production less than would be expected from their additive effects alone. We expect that both biological limits to stress responses and inhibition of H_2O_2 degradation and the associated reactive oxygen species contribute to this. Further interactive effects among H_2O_2, NPs, light, and temperature highlight the importance of introducing a specific dose of H_2O_2 that suits the local conditions for an effective cyanoHAB control. Considering the potentially broad distribution of NPs in the aquatic environment, we suggest that future investigations focus on chronic effects of polystyrene nanoparticles and H_2O_2 on cyanobacteria: local cyanobacteria may acclimate or evolve to tolerate NP pollution, which could change the interactive effects of H_2O_2 on cyanoHABs.

ASSOCIATED CONTENT

Supporting Information

The Supporting Information is available free of charge at https://pubs.acs.org/doi/10.1021/acsestwater.1c00090.

Absorbance spectra of *M. aeruginosa* (Figure S1), linear relationship between the OD and cell density of *M. aeruginosa* (Figure S2), systematic illustration of the platform setup (Figure S3), change in *M. aeruginosa* abundance over time at different H_2O_2 concentrations (Figure S4), change in H_2O_2 concentrations over time at different initial H_2O_2 doses (Figure S5), cell density of *M. aeruginosa* after exposure for 72 h with respect to multiple H_2O_2, nanoplastic, light, and temperature levels (Figure S6), MC-LR and MC-dmLR concentrations of *M. aeruginosa* after exposure for 72 h (Figure S7), D_h of PS-NH_2 at 50, 100, and 150 mg L^{-1} in the presence of different H_2O_2 concentrations (Figure S8), summary statistics for the linear regression model of cell abundance versus four stressors, excluding treatments with the highest NPs and H_2O_2 levels (Table S1), and summary statistics for the linear regression model of microcystin production versus four stressors (Table S2) (PDF)

AUTHOR INFORMATION

Corresponding Authors

David Sinton − *Department of Mechanical and Industrial Engineering, University of Toronto, Toronto, ON M5S 3G8, Canada;* orcid.org/0000-0003-2714-6408; Email: sinton@mie.utoronto.ca

Chelsea M. Rochman − *Department of Ecology and Evolutionary Biology, University of Toronto, Toronto, ON M5S 3B2, Canada;* orcid.org/0000-0002-7624-711X; Email: chelsea.rochman@utoronto.ca

Authors

Yawen Guo − *Department of Mechanical and Industrial Engineering, University of Toronto, Toronto, ON M5S 3G8, Canada*

Anna M. O'Brien − *Department of Ecology and Evolutionary Biology, University of Toronto, Toronto, ON M5S 3B2, Canada*

Tiago F. Lins − *Department of Mechanical and Industrial Engineering, University of Toronto, Toronto, ON M5S 3G8, Canada*

René Sahba Shahmohamadloo − *School of Environmental Sciences, University of Guelph, Guelph, ON N1G 2W1, Canada;* orcid.org/0000-0002-5373-9808

Xavier Ortiz Almirall − *School of Environmental Studies, Queen's University, Kingston, ON K7L 3N6, Canada*

Complete contact information is available at: https://pubs.acs.org/10.1021/acsestwater.1c00090

Author Contributions

Y.G., A.M.O., T.F.L., D.S., and C.M.R. conceived of and designed experiments, with support from R.S.S. and X.O.A. on alga-specific methods. Y.G. executed the experiments, and Y.G., R.S.S., and X.O.A. processed samples. Y.G. analyzed the data and provided the first draft of the manuscript, and Y.G., A.M.O., T.F.L., C.M.R., and D.S. revised the manuscript. All authors have given approval to the final version of the manuscript.

Notes

The authors declare no competing financial interest.

■ ACKNOWLEDGMENTS

This work was primarily supported by the Strategic Projects Grant Program of the Natural Science and Engineering Research Council of Canada (NSERC, to D.S. and C.M.R., STPGP 506882). Other funding included an E. W. R. Steacie Memorial Fellowship (D.S.) and the Canada Research Chairs Program (D.S.). Some equipment used was supported by 3D (Diet, Digestive Tract, and Disease) Centre, which is funded by the Canadian Foundation for Innovation and Ontario Research Fund (Projects 19442 and 30961).

■ REFERENCES

(1) Carmichael, W. W.; Boyer, G. L. Health impacts from cyanobacteria harmful algae blooms: Implications for the north American great lakes. *Harmful Algae* **2016**, *54*, 194−212.

(2) Huisman, J.; Codd, G. A.; Paerl, H. W.; Ibelings, B. W.; Verspagen, J. M. H.; Visser, P. M. Cyanobacterial blooms. *Nat. Rev. Microbiol.* **2018**, *16* (8), 471−483.

(3) Paerl, H. W.; Paul, V. J. Climate change: links to global expansion of harmful cyanobacteria. *Water Res.* **2012**, *46* (5), 1349−1363.

(4) Scheffer, M.; Hosper, S.H.; Meijer, M-L.; Moss, B.; Jeppesen, E. Alternative equilibria in shallow lakes. *Trends in Ecology & Evolution* **1993**, *8* (8), 275−279.

(5) Paerl, H. W.; Otten, T. G. Harmful cyanobacterial blooms: causes, conse- quences, and controls. *Microb. Ecol.* **2013**, *65* (4), 995−1010.

(6) Merel, S.; Walker, D.; Chicana, R.; Snyder, S.; Baures, E.; Thomas, O. State of knowledge and concerns on cyanobacterial blooms and cyanotoxins. *Environ. Int.* **2013**, *59*, 303−327.

(7) Paerl, H. Mitigating toxic planktonic cyanobacterial blooms in aquatic ecosystems facing increasing anthropogenic and climatic pressures. *Toxins* **2018**, *10* (2), 76.

(8) Yang, Z.; Buley, R. P.; Fernandez-Figueroa, E. G.; Barros, M. U.G.; Rajendran, S.; Wilson, A. E. Hydrogen peroxide treatment promotes chlorophytes over toxic cyanobacteria in a hyper-eutrophic aquaculture pond. *Environ. Pollut.* **2018**, *240*, 590−598.

(9) Matthijs, H. C.P.; Visser, P. M.; Reeze, B.; Meeuse, J.; Slot, P. C.; Wijn, G.; Talens, R.; Huisman, J. Selective suppression of harmful cyanobacteria in an entire lake with hydrogen peroxide. *Water Res.* **2012**, *46* (5), 1460−1472.

(10) Matthijs, H. C. P.; Jancula, D.; Visser, P. M.; Marsalek, B. Existing and emerging cyanocidal compounds: new perspectives for cyanobacterial bloom mitigation. *Aquat. Ecol.* **2016**, *50* (3), 443−460.

(11) Cooper, W. J.; Zepp, R. G. Hydrogen peroxide decay in waters with suspended soils: evidence for biologically mediated processes. *Can. J. Fish. Aquat. Sci.* **1990**, *47* (5), 888−893.

(12) Wong, G. T.F.; Dunstan, W. M.; Kim, D.-B. The decomposition of hydrogen peroxide by marine phytoplankton. *Oceanol. Acta* **2003**, *26* (2), 191−198.

(13) Hakkinen, P. J; Anesio, A. M; Graneli, W. Hydrogen peroxide distribution, production, and decay in boreal lakes. *Can. J. Fish. Aquat. Sci.* **2004**, *61* (8), 1520−1527.

(14) Drabkova, M.; Admiraal, W.; Marsalek, B. Combined exposure to hydrogen peroxide and light selective effects on cyanobacteria, green algae, and diatoms. *Environ. Sci. Technol.* **2007**, *41* (1), 309−314.

(15) Drábková, M.; Matthijs, H. C. P.; Admiraal, W.; Maršálek, B. Selective effects of h 2 o 2 on cyanobacterial photosynthesis. *Photosynthetica* **2007**, *45* (3), 363−369.

(16) Barrington, D. J.; Ghadouani, A. Application of hydrogen peroxide for the removal of toxic cyanobacteria and other phytoplankton from wastewater. *Environ. Sci. Technol.* **2008**, *42* (23), 8916−8921.

(17) Sinha, A. K.; Eggleton, M. A.; Lochmann, R. T. An environmentally friendly approach for mitigating cyanobacterial bloom and their toxins in hypereutrophic ponds: Potentiality of a newly developed granular hydrogen peroxide-based compound. *Sci. Total Environ.* **2018**, *637*−*638*, 524−537.

(18) Bauza, L.; Aguilera, A.; Echenique, R.; Andrinolo, D.; Giannuzzi, L. Application of hydrogen peroxide to the control of eutrophic lake systems in laboratory assays. *Toxins* **2014**, *6* (9), 2657−2675.

(19) Liu, M.; Shi, X.; Chen, C.; Yu, L.; Sun, C. Responses of microcystis colonies of different sizes to hydrogen peroxide stress. *Toxins* **2017**, *9* (10), 306.

(20) Folt, C. L.; Chen, C. Y.; Moore, M. V.; Burnaford, J. Synergism and antagonism among multiple stressors. *Limnol. Oceanogr.* **1999**, *44* (3part2), 864−877.

(21) Jackson, M. C.; Loewen, C. J. G.; Vinebrooke, R. D.; Chimimba, C. T. Net effects of multiple stressors in freshwater ecosystems: a meta-analysis. *Global Change Biology* **2016**, *22* (1), 180−189.

(22) Schinegger, R.; Palt, M.; Segurado, P.; Schmutz, S. Untangling the effects of multiple human stressors and their impacts on fish assemblages in european running waters. *Sci. Total Environ.* **2016**, *573*, 1079−1088.

(23) Segner, H.; Schmitt-Jansen, M.; Sabater, S. Assessing the impact of multiple stressors on aquatic biota: the receptor's side matters. *Environ. Sci. Technol.* **2014**, *48* (14), 7690−7696.

(24) Romero, F.; Sabater, S.; Timoner, X.; Acuna, V. Multistressor effects on river biofilms under global change conditions. *Sci. Total Environ.* **2018**, *627*, 1−10.

(25) Kuzmanovic, M.; Ginebreda, A.; Petrovic, M.; Barcelo, D. Risk assessment-based prioritization of 200 organic micropollutants in 4 iberian rivers. *Sci. Total Environ.* **2015**, *503*−*504*, 289−299.

(26) da Costa, J. P.; Santos, P. S.M.; Duarte, A. C.; Rocha-Santos, T. (nano) plastics in the environment−sources, fates and effects. *Sci. Total Environ.* **2016**, *566-567*, 15−26.

(27) Mattsson, K.; Jocic, S.; Doverbratt, I.; Hansson, L.-A. Nanoplastics in the aquatic environment. *Microplastic Contamination in Aquatic Environments*; Elsevier, 2018; pp 379−399.

(28) Koelmans, A. A.; Besseling, E.; Shim, W. J. Nanoplastics in the aquatic environment. Critical review. *Marine anthropogenic litter*; Springer: Cham, Switzerland, 2015; pp 325−340.
(29) Alimi, O. S.; Farner Budarz, J.; Hernandez, L. M.; Tufenkji, N. Microplastics and nanoplastics in aquatic environments: aggregation, deposition, and enhanced contaminant transport. *Environ. Sci. Technol.* **2018**, *52* (4), 1704−1724.
(30) Chae, Y.; An, Y.-J. Effects of micro-and nanoplastics on aquatic ecosystems: Current research trends and perspectives. *Mar. Pollut. Bull.* **2017**, *124* (2), 624−632.
(31) Holloczki, O.; Gehrke, S. Can nanoplastics alter cell membranes? *ChemPhysChem* **2020**, *21* (1), 9−12.
(32) Yang, Y.; Guo, Y.; O'Brien, A. M.; Lins, T. F.; Rochman, C. M.; Sinton, D. Biological responses to climate change and nanoplastics are altered in concert: Full-factor screening reveals effects of multiple stressors on primary producers. *Environ. Sci. Technol.* **2020**, *54* (4), 2401−2410.
(33) Redondo-Hasselerharm, P. E.; Gort, G.; Peeters, E. T. H. M.; Koelmans, A. A. Nano-and microplastics affect the composition of freshwater benthic communities in the long term. *Sci. Adv.* **2020**, *6* (5), eaay4054.
(34) Lee, W. S.; Cho, H.-J.; Kim, E.; Huh, Y. H.; Kim, H.-J.; Kim, B.; Kang, T.; Lee, J.-S.; Jeong, J. Bioaccumulation of polystyrene nanoplastics and their effect on the toxicity of au ions in zebrafish embryos. *Nanoscale* **2019**, *11* (7), 3173−3185.
(35) Ma, Y.; Huang, A.; Cao, S.; Sun, F.; Wang, L.; Guo, H.; Ji, R. Effects of nanoplastics and microplastics on toxicity, bioaccumulation, and environmental fate of phenanthrene in fresh water. *Environ. Pollut.* **2016**, *219*, 166−173.
(36) Jeong, C.-B.; Kang, H.-M.; Lee, Y. H.; Kim, M.-S.; Lee, J.-S.; Seo, J. S.; Wang, M.; Lee, J.-S. Nanoplastic ingestion enhances toxicity of persistent organic pollutants (pops) in the monogonont rotifer brachionus koreanus via multixenobiotic resistance (mxr) disruption. *Environ. Sci. Technol.* **2018**, *52* (19), 11411−11418.
(37) Avio, C. G.; Gorbi, S.; Milan, M.; Benedetti, M.; Fattorini, D.; d'Errico, G.; Pauletto, M.; Bargelloni, L.; Regoli, F. Pollutants bioavailability and toxicological risk from microplastics to marine mussels. *Environ. Pollut.* **2015**, *198*, 211−222.
(38) Zhang, Q.; Qu, Q.; Lu, T.; Ke, M.; Zhu, Y.; Zhang, M.; Zhang, Z.; Du, B.; Pan, X.; Sun, L.; Qian, H.; et al. The combined toxicity effect of nanoplastics and glyphosate on microcystis aeruginosa growth. *Environ. Pollut.* **2018**, *243*, 1106−1112.
(39) Trevisan, R.; Voy, C.; Chen, S.; Di Giulio, R. T. Nanoplastics de- crease the toxicity of a complex pah mixture but impair mitochondrial energy production in developing zebrafish. *Environ. Sci. Technol.* **2019**, *53* (14), 8405−8415.
(40) Feng, L.-J.; Sun, X.-D.; Zhu, F.-P.; Feng, Y.; Duan, J.-L.; Xiao, F.; Li, X.-Y.; Shi, Y.; Wang, Q.; Sun, J.-W.; Liu, X.-Y.; Liu, J.-Q.; Zhou, L.-L.; Wang, S.-G.; Ding, Z.; Tian, H.; Galloway, T. S.; Yuan, X.-Z. Nanoplastics promote microcystin synthesis and release from cyanobacterial microcystis aeruginosa. *Environ. Sci. Technol.* **2020**, *54*, 3386−3394.
(41) Feng, L.-J.; Li, J.-W.; Xu, E. G.; Sun, X.-D.; Zhu, F.-P.; Ding, Z.; Tian, H.; Dong, S.-S.; Xia, P.-F.; Yuan, X.-Z. Short-term exposure to positively charged polystyrene nanoparticles causes oxidative stress and membrane destruction in cyanobacteria. *Environ. Sci.: Nano* **2019**, *6* (10), 3072−3079.
(42) Pikuda, O.; Xu, E. G.; Berk, D.; Tufenkji, N. Toxicity assessments of micro-and nanoplastics can be confounded by preservatives in commercial formulations. *Environ. Sci. Technol. Lett.* **2019**, *6* (1), 21−25.
(43) Shen, M.; Zhang, Y.; Zhu, Y.; Song, B.; Zeng, G.; Hu, D.; Wen, X.; Ren, X. Recent advances in toxicological research of nanoplastics in the environment: A review. *Environ. Pollut.* **2019**, *252*, 511−521.
(44) Pinto da Costa, J.; Reis, V.; Paco, A.; Costa, M.; Duarte, A. C.; Rocha-Santos, T. Micro (nano) plastics−Analytical challenges towards risk evaluation. *TrAC, Trends Anal. Chem.* **2019**, *111*, 173−184.
(45) Wagner, S.; Reemtsma, T. Things we know and don't know about nanoplastic in the environment. *Nat. Nanotechnol.* **2019**, *14* (4), 300−301.
(46) Koelmans, A. A.; Mohamed Nor, N. H.; Hermsen, E.; Kooi, M.; Mintenig, S. M.; De France, J. Microplastics in freshwaters and drinking water: critical review and assessment of data quality. *Water Res.* **2019**, *155*, 410−422.
(47) Hidalgo-Ruz, V.; Gutow, L.; Thompson, R. C.; Thiel, M. Microplastics in the marine environment: a review of the methods used for identification and quantification. *Environ. Sci. Technol.* **2012**, *46* (6), 3060−3075.
(48) Lins, T. F. Unpublished work, 2021, University of Toronto, Toronto, ON.
(49) Lin, W.; Jiang, R.; Hu, S.; Xiao, X.; Wu, J.; Wei, S.; Xiong, Y.; Ouyang, G. Investigating the toxicities of different functionalized polystyrene nanoplastics on Daphnia magna. *Ecotoxicol. Environ. Saf.* **2019**, *180*, 509−516.
(50) Della Torre, C.; Bergami, E.; Salvati, A.; Faleri, C.; Cirino, P.; Dawson, K. A.; Corsi, I. Accumulation and embryotoxicity of polystyrene nanoparticles at early stage of development of sea urchin embryos paracentrotus lividus. *Environ. Sci. Technol.* **2014**, *48* (20), 12302−12311.
(51) Shahmohamadloo, R. S.; Ortiz Almirall, X.; Holeton, C.; Chong-Kit, R.; Poirier, D. G.; Bhavsar, S. P.; Sibley, P. K. An efficient and affordable laboratory method to produce and sustain high concentrations of microcystins by microcystis aeruginosa. *MethodsX* **2019**, *6*, 2521−2535.
(52) Tanabe, Y.; Hodoki, Y.; Sano, T.; Tada, K.; Watanabe, M. M. Adaptation of the freshwater bloom-forming cyanobacterium microcystis aeruginosa to brackish water is driven by recent horizontal transfer of sucrose genes. *Front. Microbiol.* **2018**, *9*, 1150.
(53) *Guidelines for safe recreational water environments: Coastal and fresh waters*, Vol. *1*; World Health Organization, 2003.
(54) Wyman, M.; Fay, P. Underwater light climate and the growth and pigmentation of plank- tonic blue-green algae (cyanobacteria) i. the influence of light quantity. *Proc. R. Soc. B* **1986**, *227* (1248), 367−380.
(55) Wiedner, C.; Visser, P. M.; Fastner, J.; Metcalf, J. S.; Codd, G. A.; Mur, L. R. Effects of light on the microcystin content of microcystis strain pcc 7806. *Appl. Environ. Microbiol.* **2003**, *69* (3), 1475−1481.
(56) Van der Westhuizen, A. J.; Eloff, J. N. Effect of temperature and light on the toxicity and growth of the blue-green alga microcystis aeruginosa (uv-006). *Planta* **1985**, *163* (1), 55−59.
(57) Xie, L.; Rediske, R. R.; Gillett, N. D.; O'Keefe, J. P.; Scull, B.; Xue, Q. The impact of environmental parameters on microcystin production in dial- ysis bag experiments. *Sci. Rep.* **2016**, *6*, 38722.
(58) Davis, T. W.; Berry, D. L.; Boyer, G. L.; Gobler, C. J. The effects of temperature and nutrients on the growth and dynamics of toxic and non-toxic strains of microcystis during cyanobacteria blooms. *Harmful Algae* **2009**, *8* (5), 715−725.
(59) Rowe, M. D.; Anderson, E. J.; Wynne, T. T.; Stumpf, R. P.; Fanslow, D. L.; Kijanka, K.; Vander- ploeg, H. A.; Strickler, J. R.; Davis, T. W. Vertical distribution of buoyant microcystis blooms in a lagrangian particle tracking model for short-term forecasts in lake erie. *J. Geophys. Res.: Oceans* **2016**, *121* (7), 5296−5314.
(60) Puddick, J.; Prinsep, M. R.; Wood, S. A.; Cary, S. C.; Hamilton, D. P. Modulation of microcystin congener abundance following nitrogen depletion of a microcystis batch culture. *Aquat. Ecol.* **2016**, *50* (2), 235−246.
(61) Bouaïcha, N.; Miles, C. O.; Beach, D. G.; Labidi, Z.; Djabri, A.; Benayache, N. Y.; Nguyen-Quang, T. Structural diversity, characterization and toxicology of microcystins. *Toxins* **2019**, *11* (12), 714.
(62) Ortiz, X.; Korenkova, E.; Jobst, K. J.; MacPherson, K. A.; Reiner, E. J. A high throughput targeted and non-targeted method for the analysis of microcystins and anatoxin-a using on-line solid phase extraction coupled to liquid chromatography− quadrupole time-of-flight high resolution mass spectrometry. *Anal. Bioanal. Chem.* **2017**, *409* (21), 4959−4969.

https://doi.org/10.1021/acsestwater.1c00090
ACS EST Water 2021, 1, 1596−1607

(63) van Rossum, G. Python tutorial. Technical Report CS-R9526; Centrum voor Wiskunde en Informatica (CWI): Amsterdam, 1995.
(64) Waskom, M.; Seaborn Development Team. mwaskom/seaborn, September 2020. DOI: 10.5281/zenodo.592845.
(65) Imai, H.; Chang, K.-H.; Kusaba, M.; Nakano, S.-i. Temperature-dependent dominance of microcystis (cyanophyceae) species: M. aeruginosa and m. wesenbergii. *J. Plankton Res.* **2008**, *31* (2), 171−178.
(66) Bui, T.; Dao, T.-S.; Vo, T.-G.; Lurling, M. Warming affects growth rates and microcystin production in tropical bloom-forming microcystis strains. *Toxins* **2018**, *10* (3), 123.
(67) Wan, J.-K.; Chu, W.-L.; Kok, Y.-Y.; Lee, C.-S. Distribution of microplastics and nanoplastics in aquatic ecosystems and their impacts on aquatic organisms, with emphasis on microalgae. In *Reviews of Environmental Contamination and Toxicology*, Vol. *246*; Springer, 2018; pp 133−158.
(68) Anguissola, S.; Garry, D.; Salvati, A.; O'Brien, P. J.; Dawson, K. A. High content analysis provides mechanistic insights on the pathways of toxicity induced by amine-modified polystyrene nanoparticles. *PLoS One* **2014**, *9* (9), e108025.
(69) Bergami, E.; Pugnalini, S.; Vannuccini, M. L.; Manfra, L.; Faleri, C.; Savorelli, F.; Dawson, K. A.; Corsi, I. Long-term toxicity of surface-charged polystyrene nanoplastics to marine planktonic species dunaliella tertiolecta and artemia franciscana. *Aquat. Toxicol.* **2017**, *189*, 159−169.
(70) Kelpsiene, E.; Torstensson, O.; Ekvall, M. T.; Hansson, L.-A.; Cedervall, T. Long-term exposure to nanoplastics reduces lifetime in daphnia magna. *Sci. Rep.* **2020**, *10* (1), 5979.
(71) Zhang, C.; Chen, X.; Wang, J.; Tan, L. Toxic effects of microplastic on marine microalgae skeletonema costatum: interactions between microplastic and algae. *Environ. Pollut.* **2017**, *220*, 1282−1288.
(72) Bhattacharya, P.; Lin, S.; Turner, J. P.; Ke, P. C. Physical adsorption of charged plastic nanoparticles affects algal photosynthesis. *J. Phys. Chem. C* **2010**, *114* (39), 16556−16561.
(73) Bellingeri, A.; Bergami, E.; Grassi, G.; Faleri, C.; Redondo-Hasselerharm, P.; Koelmans, A. A.; Corsi, I. Combined effects of nanoplastics and copper on the freshwater alga raphidocelis subcapitata. *Aquat. Toxicol.* **2019**, *210*, 179−187.
(74) Kogel, T.; Bjorøy, Ør.; Toto, B.; Bienfait, A. M.; Sanden, M. Micro-and nanoplastic toxicity on aquatic life: Determining factors. *Sci. Total Environ.* **2020**, *709*, 136050.
(75) Lee, K.-W.; Shim, W. J.; Kwon, O. Y.; Kang, J.-H. Size-dependent effects of micro polystyrene particles in the marine copepod tigriopus japonicus. *Environ. Sci. Technol.* **2013**, *47* (19), 11278−11283.
(76) Kokalj, A. J.; Kunej, U.; Skalar, T. Screening study of four environmentally relevant microplastic pollutants: uptake and effects on daphnia magna and artemia franciscana. *Chemosphere* **2018**, *208*, 522−529.
(77) Yu, S.; Shen, M.; Li, S.; Fu, Y.; Zhang, D.; Liu, H.; Liu, J. Aggregation kinetics of different surface-modified polystyrene nanoparticles in monovalent and divalent electrolytes. *Environ. Pollut.* **2019**, *255*, 113302.
(78) Brewer, A.; Dror, I.; Berkowitz, B. The Mobility of Plastic Nanoparticles in Aqueous and Soil Environments: A Critical Review. *ACS ES&T Water* **2021**, *1* (1), 48−57.
(79) Song, Z.; Yang, X.; Chen, F.; Zhao, F.; Zhao, Y.; Ruan, L.; Wang, Y.; Yang, Y. Fate and transport of nanoplastics in complex natural aquifer media: Effect of particle size and surface functionalization. *Sci. Total Environ.* **2019**, *669*, 120−128.
(80) Oriekhova, O.; Stoll, S. Heteroaggregation of nanoplastic particles in the presence of inorganic colloids and natural organic matter. *Environ. Sci.: Nano* **2018**, *5* (3), 792−799.
(81) Manfra, L.; Rotini, A.; Bergami, E.; Grassi, G.; Faleri, C.; Corsi, I. Comparative ecotoxicity of polystyrene nanoparticles in natural seawater and reconstituted seawater using the rotifer Brachionus plicatilis. *Ecotoxicol. Environ. Saf.* **2017**, *145*, 557−563.
(82) Wu, J.; Jiang, R.; Lin, W.; Ouyang, G. Effect of salinity and humic acid on the aggregation and toxicity of polystyrene nanoplastics with different functional groups and charges. *Environ. Pollut.* **2019**, *245*, 836−843.
(83) Frankel, R.; Ekvall, M. T.; Kelpsiene, E.; Hansson, L.-A.; Cedervall, T. Controlled protein mediated aggregation of polystyrene nanoplastics does not reduce toxicity towards Daphnia magna. *Environ. Sci.: Nano* **2020**, *7* (5), 1518−1524.
(84) Li, Y.; Wang, X.; Fu, W.; Xia, X.; Liu, C.; Min, J.; Zhang, W.; Crittenden, J. C. Interactions between nano/micro plastics and suspended sediment in water: Implications on aggregation and settling. *Water Res.* **2019**, *161*, 486−495.
(85) Spoof, L.; Jaakkola, S.; Vazic, T.; Haggqvist, K.; Kirkkala, T.; Ventela, A.-M.; Kirkkala, T.; Svircev, Z.; Meriluoto, J. Elimination of cyanobacteria and microcystins in irrigation water—effects of hydrogen peroxide treatment. *Environ. Sci. Pollut. Res.* **2020**, *27* (8), 8638−8652.
(86) Papadimitriou, T.; Kormas, K.; Dionysiou, D. D.; Laspidou, C. Using H_2O_2 treatments for the degradation of cyanobacteria and microcystins in a shallow hypertrophic reservoir. *Environ. Sci. Pollut. Res.* **2016**, *23* (21), 21523−21535.
(87) Tanabe, Y.; Hodoki, Y.; Sano, T.; Tada, K.; Watanabe, M. M. Adaptation of the freshwater bloom-forming cyanobacterium microcystis aeruginosa to brackish water is driven by recent horizontal transfer of sucrose genes. *Front. Microbiol.* **2018**, *9*, 1150.
(88) Crain, C. M.; Kroeker, K.; Halpern, B. S. Interactive and cumulative effects of multiple human stressors in marine systems. *Ecology Letters* **2008**, *11* (12), 1304−1315.
(89) Piggott, J. J.; Townsend, C. R.; Matthaei, C. D. Reconceptualizing synergism and antagonism among multiple stressors. *Ecology and Evolution* **2015**, *5* (7), 1538−1547.
(90) CHRISTENSEN, M. R.; GRAHAM, M. D.; VINEBROOKE, R. D.; FINDLAY, D. L.; PATERSON, M. J.; TURNER, M. A. Multiple anthropogenic stressors cause ecological surprises in boreal lakes. *Global Change Biology* **2006**, *12* (12), 2316−2322.
(91) Blanck, H. A critical review of procedures and approaches used for assessing pollution- induced community tolerance (pict) in biotic communities. *Hum. Ecol. Risk Assess.* **2002**, *8* (5), 1003−1034.
(92) Russell, A. D. Similarities and differences in the responses of microorganisms to biocides. *Journal of antimicrobial chemotherapy* **2003**, *52* (5), 750−763.
(93) Chang, C.-W.; Huo, X.; Lin, T.-F. Exposure of Microcystis aeruginosa to hydrogen peroxide and titanium dioxide under visible light conditions: Modeling the impact of hydrogen peroxide and hydroxyl radical on cell rupture and microcystin degradation. *Water Res.* **2018**, *141*, 217−226.
(94) Saha, D.; Desipio, M. M.; Hoinkis, T. J.; Smeltz, E. J.; Thorpe, R.; Hensley, D. K.; Fischer-Drowos, S. G.; Chen, J. Influence of hydrogen peroxide in enhancing photocatalytic activity of carbon nitride under visible light: An insight into reaction intermediates. *J. Environ. Chem. Eng.* **2018**, *6* (4), 4927−4936.
(95) Rincon, A.-G.; Pulgarin, C. Effect of ph, inorganic ions, organic matter and h2o2 on e. coli k12 photocatalytic inactivation by tio2: implications in solar water disinfection. *Appl. Catal., B* **2004**, *51* (4), 283−302.
(96) Robarts, R. D.; Zohary, T. Temperature effects on photosynthetic capacity, respiration, and growth rates of bloom-forming cyanobacteria. *N. Z. J. Mar. Freshwater Res.* **1987**, *21* (3), 391−399.
(97) Fu, F.-X.; Warner, M. E.; Zhang, Y.; Feng, Y.; Hutchins, D. A. Effects of increased temperature and co2 on photosynthesis, growth, and elemental ratios in marine synechococcus and prochlorococcus (cyanobacteria) 1. *J. Phycol.* **2007**, *43* (3), 485−496.
(98) Thomas, M. K.; Litchman, E. Effects of temperature and nitrogen availability on the growth of invasive and native cyanobacteria. *Hydrobiologia* **2016**, *763* (1), 357−369.
(99) Huisman, J.; Sharples, J.; Stroom, J. M.; Visser, P. M.; Kardinaal, W. E. A.; Verspagen, J. M. H.; Sommeijer, B. Changes in turbulent mixing shift competition for light between phytoplankton species. *Ecology* **2004**, *85* (11), 2960−2970.

(100) Hesse, K.; Dittmann, E.; Börner, T. Consequences of impaired microcystin production for light-dependent growth and pigmentation of microcystis aeruginosa pcc 7806. *FEMS Microbiol. Ecol.* **2001**, *37* (1), 39−43.
(101) Tomioka, N.; Imai, A.; Komatsu, K. Effect of light availability on microcystis aeruginosa blooms in shallow hypereutrophic lake kasumigaura. *J. Plankton Res.* **2011**, *33* (8), 1263−1273.
(102) Watanabe, M. F.; Oishi, S. Effects of environmental factors on toxicity of a cyanobacterium (microcystis aeruginosa) under culture conditions. *Appl. Environ. Microbiol.* **1985**, *49* (5), 1342−1344.
(103) Chorus, I. *Cyanotoxins: occurrence, causes, consequences*; Springer Science & Business Media, 2012.
(104) Rapala, J.; Sivonen, K. Assessment of environmental conditions that favor hepatotoxic and neurotoxic anabaena spp. strains cultured under light limitation at different temperatures. *Microb. Ecol.* **1998**, *36* (2), 181−192.
(105) de Figueiredo, D. R.; Azeiteiro, U. M.; Esteves, S. M.; Goncalves, F. J.M.; Pereira, M. J. Microcystin-producing blooms—a serious global public health issue. *Ecotoxicol. Environ. Saf.* **2004**, *59* (2), 151−163.

https://doi.org/10.1021/acsestwater.1c00090
ACS EST Water 2021, 1, 1596−1607